

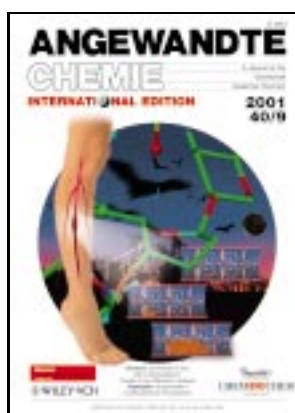
# ANGEWANDTE CHEMIE

A Journal of the  
Gesellschaft  
Deutscher Chemiker

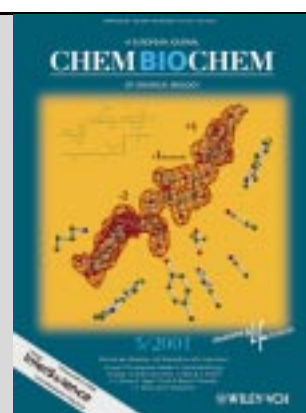
INTERNATIONAL EDITION

2001  
40/9

Pages 1557 – 1786



*ChemBioChem* 5/2001 is bound  
in this issue of *Angewandte Chemie*.



## COVER PICTURE

The cover picture shows how thrombosis occurs in the deep veins of the lower limbs. Stasis, which results from slow and turbulent blood flow, combined with hypercoagulation, caused, for example, by a surgical procedure, may result in thrombus formation. The synthetic sulfated pentasaccharide shown in part is a potent antithrombotic compound that exerts its effect by activation of the plasma protein antithrombin III. Conformationally locked monosaccharides have now been synthesized to demonstrate that L-iduronic acid, one part of the pentasaccharide, must adopt an unusual distorted conformation to activate antithrombin III. Such conformational effects might be relevant in explaining the unique biological properties of glycosaminoglycans that contain L-iduronic acid. In the background of the picture, a flight of vampire bats is attracted by the pentasaccharide. Vampire was the name given to South American blood-sucking bats (Latin name: *desmodus rotundus*) in 1761 by the French naturalist Georges Louis Leclerc Comte de Buffon (1707–1788). These bats are known to attack cattle and, very rarely, sleeping human beings. Although their saliva has been shown to contain an anticoagulant compound, they would also be happy to benefit from the pentasaccharide mentioned above, to suck the blood out of the vein more easily. More details about this compound which would be helpful to vampire bats are reported by Petitou, Sinaÿ et al. on p. 1670 ff.

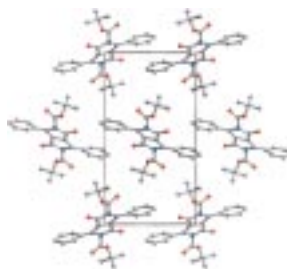


**The teamwork between carbohydrate chemistry and total synthesis** is surely one of the most exciting aspects of organic chemistry. In this review the contributions made by the principal author's research group in the areas of chemical synthesis and biological chemistry of carbohydrates are presented. Specifically, the use of carbohydrates as starting materials for total synthesis, the development of new technologies for carbohydrate synthesis, the construction of complex oligosaccharides in solution or on solid support, and the use of carbohydrate templates as scaffolds for peptide mimetics and other interesting compounds are discussed.

*Angew. Chem.* **2001**, *113*, 1624–1672

**As many materials cannot be prepared in the form of single crystals** appropriate for single-crystal X-ray diffraction, structure determination of such materials requires the use of powder X-ray diffraction data. However, the determination of crystal structures directly from powder X-ray diffraction data is associated with a number of intrinsic challenges. In recent years there has been substantial progress in the development of techniques to tackle these challenges. In addition to surveying these advances in methodology, the opportunities that now exist for exploiting powder diffraction in structure determination are highlighted with examples taken from diverse areas across the chemical and materials sciences. The picture shows the  $\beta$  phase from 1,4-diketo-2,5-di-*tert*-butoxycarbonyl-3,6-diphenylpyrrolo[3,4]pyrrole.

*Angew. Chem.* **2001**, *113*, 1674–1700



K. C. Nicolaou,\*  
H. J. Mitchell ..... 1576–1624

Adventures in Carbohydrate Chemistry:  
New Synthetic Technologies, Chemical  
Synthesis, Molecular Design, and  
Chemical Biology

**Keywords:** carbohydrates •  
glycosylation • natural products •  
synthetic methods • total synthesis

K. D. M. Harris,\* M. Tremayne,  
B. M. Kariuki ..... 1626–1651

Contemporary Advances in the Use of  
Powder X-Ray Diffraction for Structure  
Determination

**Keywords:** powder X-ray diffraction •  
structure elucidation • X-ray diffraction

## VIPs

The following communications are “Very Important Papers” in the opinion of two referees. They will be published shortly (those marked with a diamond will be published in the next issue). Short summaries of these articles can be found on the *Angewandte Chemie* homepage at the address <http://www.angewandte.com>

Cyclic Dimers of Metalloporphyrins as Tunable Hosts for Fullerenes:  
A Remarkable Effect of Rhodium(III)

J.-Y. Zheng, K. Tashiro,  
Y. Hirabayashi, K. Kinbara,  
K. Saigo,\* T. Aida,\*  
S. Sakamoto, K. Yamaguchi



Direct Observation of Surface-Controlled Self-Assembly of Coordination  
Cages by Using Atomic Force Microscopy as a Molecular Ruler

S. A. Levi, P. Guatterri,  
F. C. J. M. van Veggel,  
G. J. Vancso, E. Dalcanele,\*  
D. N. Reinhoudt\*



Probing Guest Geometry and Dynamics through Host–Guest Interactions

T. Kusukawa, M. Yoshizawa,  
M. Fujita\*



Fluorinated Bis(enyl) Ligands through Metal-Induced Dimerization of  
Fluorinated Allenes

D. Lentz,\* S. Willemsen

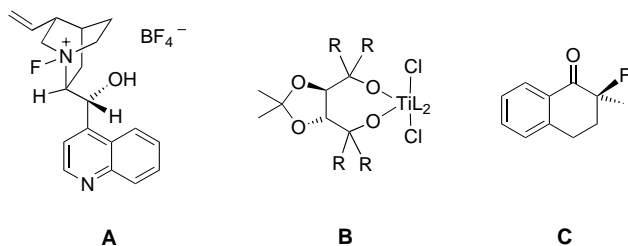
The Natural  $^{12}\text{C}/^{13}\text{C}$  Ratio Allows Classification of Terpenoid Biosynthesis  
According to the Methylerythritolphosphate or the Mevalonate Pathway:  
Dynamic Allocation of Resources in Induced Plants

A. Jux, G. Gleixner, W. Boland\*

Targeting Molecular Recognition: Exploring the Dual Role of Functional  
Pseudo-Prolines in the Design of SH3 Ligands

G. Tuchscherer,\* D. Grell,  
Y. Tatsu, P. Durieux,  
J. Fernandez-Carneado,  
B. Hengst, C. Kardinal, S. Feller\*

**Enantioselective fluorinations made easier!** Chiral *N*-fluoroammonium salts such as **A**, or chiral catalysts generated from complexes **B** (L = ligand) broaden the substrate scope for electrophilic fluorination. Starting from prochiral substrates they offer an efficient approach to chiral fluoro derivatives such as **C**. Additionally, fluorinated stereogenic centers can be generated from nucleophilic, catalytic epoxide opening.



*Angew. Chem.* **2001**, *113*, 1701–1704

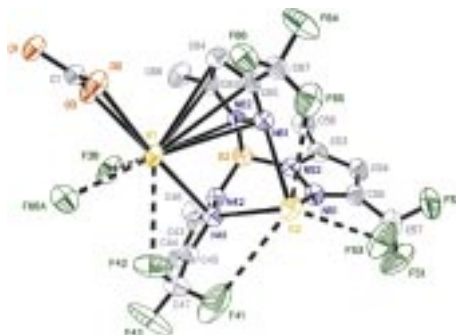
K. Muñoz\* ..... 1653–1656

Improving Enantioselective Fluorination Reactions: Chiral *N*-Fluoroammonium Salts and Transition Metal Catalysts

**Keywords:** asymmetric catalysis • asymmetric synthesis • fluoroorganic compounds • homogeneous catalysis • transition metals

**Much more versatile than previously anticipated** are the coordination modes of tris(pyrazolyl)borate ligands (scorpionates). Recent contributions in this area not only lead to a new understanding of the electronic effects, but for the first time report unusually high and low hapticities as well as novel coordination modes such as the  $\pi$  coordination of a pyrazolyl ring to potassium (see structure). Potentially useful new ligands have been made available through innovative synthetic routes.

*Angew. Chem.* **2001**, *113*, 1704–1708



F. T. Edelmann\* ..... 1656–1660

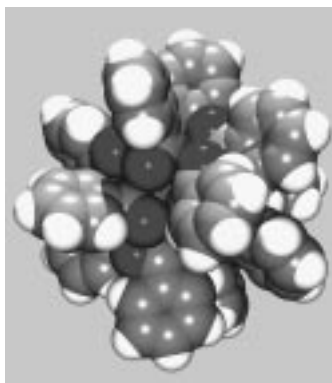
Versatile Scorpionates—New Developments in the Coordination Chemistry of Pyrazolylborate Ligands

**Keywords:** copper • iridium • pyrazolylborates • rhodium • samarium

## COMMUNICATIONS

**Esterified  $B_{12}$  icosahedra** with totally organoderivatized surfaces are obtained from the reaction of [*closo*- $B_{12}(OH)_{12}$ ] $^{2-}$  with acetic anhydride or benzoyl chloride. The resulting “closomers”, in which each cluster vertex is substituted with an organic ester moiety, can provide camouflaged modules of variable size, shape, charge, hydrophobicity, etc. and represent the first examples of this structural motif known in chemistry. The figure displays, in a space-filling representation, the result of an X-ray analysis performed with the dodecabenzoate ester derivative.

*Angew. Chem.* **2001**, *113*, 1710–1712

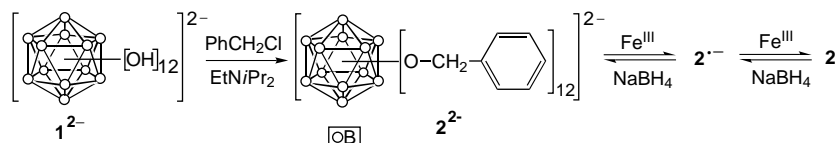


A. Maderna, C. B. Knobler, M. F. Hawthorne\* ..... 1662–1664

Twelvefold Functionalization of an Icosahedral Surface by Total Esterification of [ $B_{12}(OH)_{12}$ ] $^{2-}$ : 12(12)-Closomers

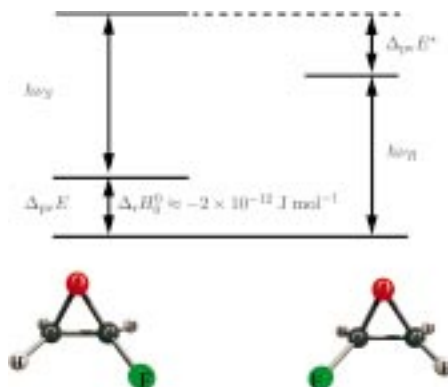
**Keywords:** boranes • boron • closomers • cluster compounds • esterification

**Per-O-benylation** of  $[closo-B_{12}(OH)_{12}]^{2-}$  (**1**<sup>2-</sup>) using benzyl chloride followed by oxidation with two equivalents of Fe<sup>III</sup> gave compound **2**, the per(benzyloxy) derivative of *hypercloso*-B<sub>12</sub>H<sub>12</sub> (see scheme). Species **2** is characterized by <sup>11</sup>B NMR and electronic spectroscopy, mass spectrometry, cyclic voltammetry, and X-ray crystallography.



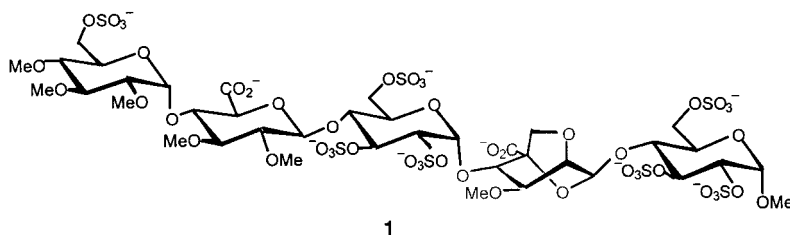
*Angew. Chem.* **2001**, *113*, 1713–1715

**In contrast to what has been accepted**, electroweak quantum chemistry predicts the heats of formation, the structures, the microwave and infrared spectra of enantiomers of chiral molecules to be different. The *R* enantiomer of fluoroxirane is calculated to be more stable than the *S* enantiomer by the minute amount of  $2 \times 10^{-12}$  J mol<sup>-1</sup>, and the relative IR frequency shifts are  $\leq 10^{-18}$  (see scheme). Nevertheless, this recently synthesized compound may prove useful for fundamental experimental tests and calculations of parity violation in chiral molecules because of its particularly simple rovibrational spectrum and its rigid cyclic structure composed of light atoms.



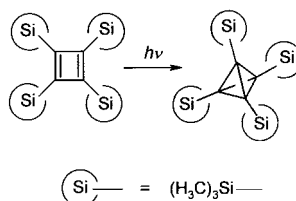
*Angew. Chem.* **2001**, *113*, 1716–1719

**Conformational flexibility of L-iduronic acid** is a key feature of this typical component of heparin. Three pentasaccharides have now been synthesized, which are analogues of the active site of heparin and in which the single L-iduronic acid is conformationally locked in either the <sup>1</sup>C<sub>4</sub>, <sup>4</sup>C<sub>1</sub>, or <sup>2</sup>S<sub>0</sub> form. Only the <sup>2</sup>S<sub>0</sub> variant **1** was able to fully activate antithrombin inhibition of the blood coagulation factor Xa.



*Angew. Chem.* **2001**, *113*, 1723–1726

**A route to unsubstituted tetrahedrane?** One option is offered by the tetrakis(trimethylsilyl) derivative, which is generated upon irradiation of the corresponding cyclobutadiene (see scheme). Tetrahedrane itself could also possibly be accessed from the tetralithiotetrahedrane by this route.



*Angew. Chem.* **2001**, *113*, 1719–1720

T. Peymann, C. B. Knobler, S. I. Khan, M. F. Hawthorne\* ..... 1664–1667

Dodeca(benzyloxy)dodecaborane, B<sub>12</sub>(OCH<sub>2</sub>Ph)<sub>12</sub>: A Stable Derivative of *hypercloso*-B<sub>12</sub>H<sub>12</sub>

**Keywords:** boranes • boron • closomers • cluster compounds • electron-deficient compounds

R. Berger, M. Quack,\* J. Stohner ..... 1667–1670

Parity Violation in Fluorooxirane

**Keywords:** ab initio calculations • chirality • electroweak quantum chemistry • oxiranes • parity violation

S. K. Das, J.-M. Mallet, J. Esnault, P.-A. Driguez, P. Duchaussoy, P. Sizun, J.-P. Héroult, J.-M. Herbert, M. Petitou,\* P. Sinaÿ\* ..... 1670–1673

Synthesis of Conformationally Locked Carbohydrates: A Skew-Boat Conformation of L-Iduronic Acid Governs the Antithrombotic Activity of Heparin

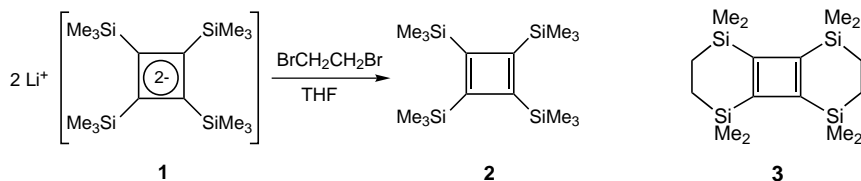
**Keywords:** blood coagulation • carbohydrates • glycosylation • heparin • molecular recognition

G. Maier,\* J. Neudert, O. Wolf ..... 1674–1675

Tetrakis(trimethylsilyl)cyclobutadiene and Tetrakis(trimethylsilyl)tetrahedrane

**Keywords:** cycloalkenes • diazo compounds • ketenimines • photochemistry • small ring systems • tetrahedranes

**In less than one minute** dianion **1** can be oxidized with 1,2-dibromoethane to give pure tetrakis(trimethylsilyl)cyclobutadiene (**2**, see scheme). The bridged cyclobutadiene derivative **6** was also similarly synthesized and characterized by X-ray crystallography; it exhibits a planar rectangular structure with localized C=C bonds.



*Angew. Chem.* **2001**, *113*, 1721–1723

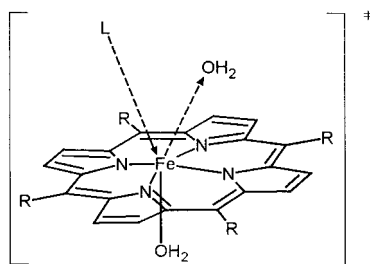
A. Sekiguchi,\* M. Tanaka, T. Matsuo,  
H. Watanabe ..... 1675–1677

From a Cyclobutadiene Dianion to a  
Cyclobutadiene: Synthesis and Structural  
Characterization of Tetrasilyl-Substituted  
Cyclobutadiene

**Keywords:** carbanions • cycloalkenes •  
oxidation • small ring systems •  
solid-state structures



**The water-exchange reactions** of three modified iron(III) porphyrins were studied in acidic medium as a function of temperature and pressure using <sup>17</sup>O NMR spectroscopic techniques. The positive activation entropies and activation volumes support a dissociative mechanism (see scheme showing the transition state; L = nucleophile, H<sub>2</sub>O, NO). A comparison with available literature data reveals that the rate and mechanism of complex-formation reactions of such metal porphyrins are controlled by the water-exchange process.



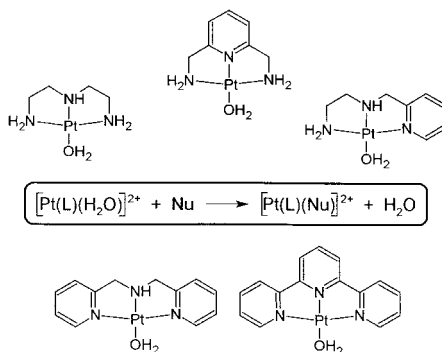
*Angew. Chem.* **2001**, *113*, 1727–1729

T. Schnieppensieper, A. Zahl,  
R. van Eldik\* ..... 1678–1680

Water Exchange Controls the Complex-  
Formation Mechanism of Water-Soluble  
Iron(III) Porphyrins: Conclusive Evidence  
for Dissociative Water Exchange from a  
High-Pressure <sup>17</sup>O NMR Study

**Keywords:** high-pressure chemistry •  
iron • NMR spectroscopy •  
porphyrinoids • water exchange

**By a factor of 10<sup>4</sup>–10<sup>5</sup>** that is how much the reactivity of Pt<sup>II</sup>(terpyridine) complexes exceeds the reactivity of the corresponding Pt<sup>II</sup>-(diene) complexes in nucleophilic substitution reactions. A systematic π-acceptor study was performed on a series of aqua complexes (see scheme) to elucidate that the source of this unusual acceleration is π conjugation!



*Angew. Chem.* **2001**, *113*, 1730–1733

D. Jaganyi, A. Hofmann,  
R. van Eldik\* ..... 1680–1683

Controlling the Lability of Square-Planar  
Pt<sup>II</sup> Complexes through Electronic  
Communication between π-Acceptor  
Ligands

**Keywords:** kinetics • N ligands •  
platinum • thermodynamics •  
tridentate ligands

**Diffusion or perfusion—this is no longer the question** for electroosmotic flow (EOF) through capillaries with fixed beds. The intraparticle EOF in capillary electrochromatography has been shown by using special NMR techniques and forms the basis for a further improvement in separation efficiency, mass sensitivity, and analysis speed. Electroosmotic perfusion phenomena in porous materials also play an important role in other areas, such as in the dewatering of waste sludge and the removal of contaminants from soil.

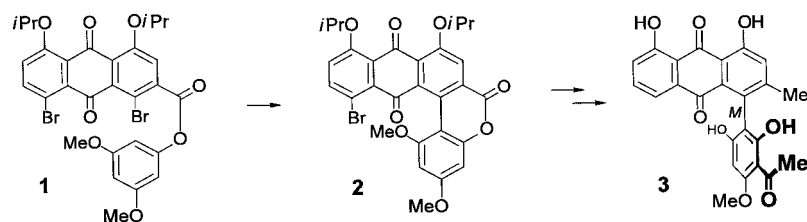
*Angew. Chem.* **2001**, *113*, 1741–1745

U. Tallarek,\* E. Rapp, H. Van As,  
E. Bayer ..... 1684–1687

Electrokinetics in Fixed Beds:  
Experimental Demonstration of  
Electroosmotic Perfusion

**Keywords:** analytical methods •  
electroosmotic flow •  
liquid chromatography • mass transfer •  
NMR spectroscopy

**The first stereoselective access to an axially chiral arylanthraquinone**, the antimalarial natural product knipholone (**3**), was achieved by application of the “lactone concept”. Key steps were the intramolecular coupling of the bromoester **1**, to give the configurationally unstable biaryl lactone **2**, and the enantioselective ring cleavage to form **3**.



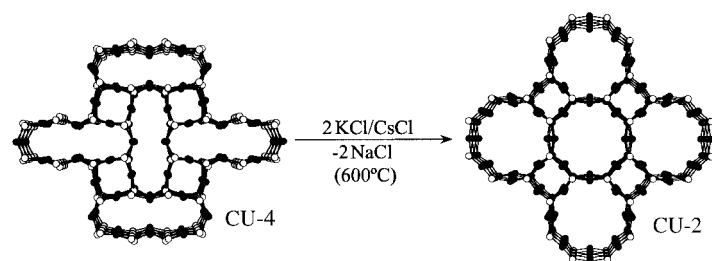
*Angew. Chem.* **2001**, *113*, 1733–1736

G. Bringmann,\* D. Menche 1687–1690

First, Atropo-Enantioselective Total Synthesis of the Axially Chiral Phenylanthraquinone Natural Products Knipholone and 6'-O-Methylknipholone

**Keywords:** atropisomerism • enantiomer resolution • natural products • quinones • total synthesis

**8-Ring and 16-ring channels** with  $5.3 \times 5.3$  Å and  $4.9 \times 17.2$  Å windows, respectively, are contained in the new CU-4 phase. The larger channel exhibits an elliptical pore structure templated by an alkali metal chloride salt. CU-4 is structurally related to CU-2 (see picture), and can be chemically modified to CU-2 by an ion-exchange reaction at 600°C.



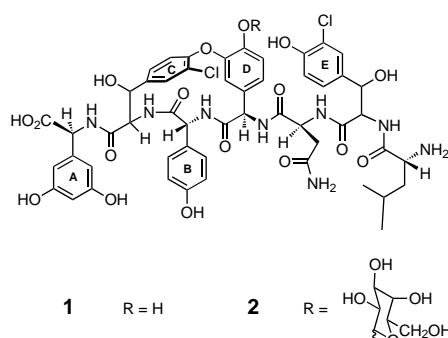
*Angew. Chem.* **2001**, *113*, 1754–1756

Q. Huang, S.-J. Hwu,\*  
X. Mo ..... 1690–1693

High-Temperature Synthesis of an Open-Framework Compound,  $\text{Na}_2\text{Cs}_2\text{Cu}_3(\text{P}_2\text{O}_7)_2\text{Cl}_2$  (CU-4), by Molten-Salt Methods

**Keywords:** cuprates • microporosity • solid-state structures • template synthesis • zeolite analogues

**A new oxyA gene replacement mutant** of *Amycolatopsis mediterranei* enabled us to isolate two peptides, SP-1132 (**1**) and SP-1294 (**2**), which only have one diaryl ether bridge. These vancomycin-type structures provide further insight into the oxidative ring-bridging steps in their biosynthesis.



*Angew. Chem.* **2001**, *113*, 1736–1739

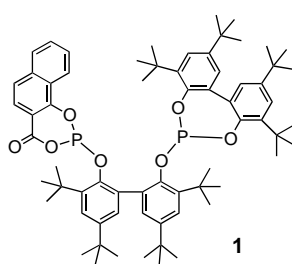
D. Bischoff, S. Pelzer, A. Hölzel,  
G. J. Nicholson, S. Stockert,  
W. Wohlleben, G. Jung,  
R. D. Süßmuth\* ..... 1693–1696

The Biosynthesis of Vancomycin-Type Glycopeptide Antibiotics—New Insights into the Cyclization Steps

**Keywords:** antibiotics • biaryls • biosynthesis • glycopeptides • structure elucidation



**Going up!** *n*-Selectivity and activity can be increased simultaneously in hydroformylation by the use of novel hybrid ligands such as **1** containing *O*-acylphosphite groups. For the first time these ligands deliver impressively *n*-selective rhodium-catalyzed hydroformylation of internal octenes, and this with an industrial relevant catalytic activity.



*Angew. Chem.* **2001**, *113*, 1739–1741

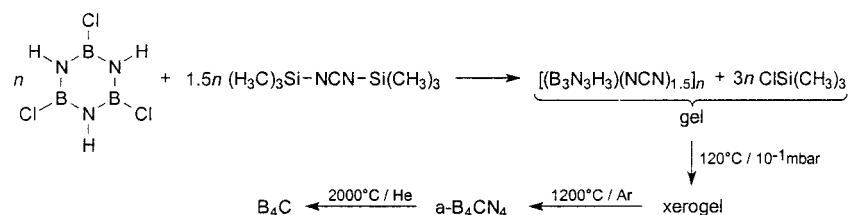
D. Selent,\* D. Hess, K.-D. Wiese,  
D. Röttger, C. Kunze,  
A. Börner\* ..... 1696–1698

New Phosphorus Ligands for the Rhodium-Catalyzed Isomerization/Hydroformylation of Internal Octenes

**Keywords:** homogeneous catalysis • hydroformylation • isomerization • P ligands • rhodium



**B-trichloroborazene** reacts with bis(trimethylsilyl)carbodiimide to form non-oxide gels (see scheme). The xerogels consist of a polymeric network of borazine rings linked by carbodiimide groups. Pyrolysis at 1200°C provides amorphous ceramics with the composition  $\text{BC}_{0.23}\text{N}_{1.1}\text{Si}_{0.05}\text{H}_{0.09} \approx \text{B}_4\text{CN}_4$ . At 2000°C pure  $\text{B}_4\text{C}$  is formed.



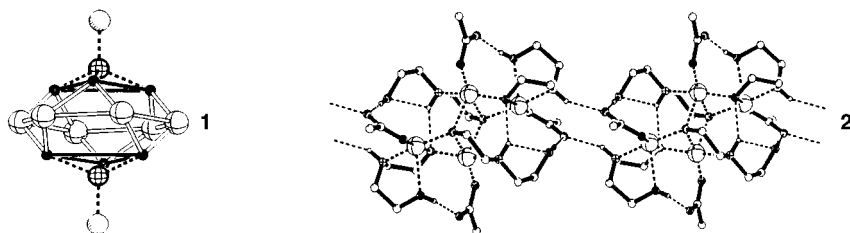
*Angew. Chem.* **2001**, *113*, 1751–1753

E. Kroke,\* K. W. Völger, A. Klonczynski, R. Riedel ..... 1698–1700

A Sol–Gel Route to  $\text{B}_4\text{C}$

**Keywords:** boron • ceramics • gels • sol–gel process

**Template effect versus hydrogen bonding** in self-assembly: As predicted, the scaffold of molecular gyroscope  $[(\text{NaBr})_2 \cap \text{Cu}_6\{(\text{2,5-Me}_2\text{C}_6\text{H}_3\text{CH}_2)\text{N}(\text{CH}_2\text{CH}_2\text{O})_2\}_6]$  (**1**) is generated from N-substituted diethanolamine together with a copper(II) salt and sodium bromide. However, we did not predict the one-dimensional coordination polymer  $[\text{Cu}_4\{\text{H}[\text{HN}(\text{CH}_2\text{CH}_2\text{O})_2]\}_4(\text{OAc})_4]$  (**2**) generated with an unsubstituted diethanolamine. The formation of **2** is a further impressive example of nature's virtuosity in using hydrogen bonds.



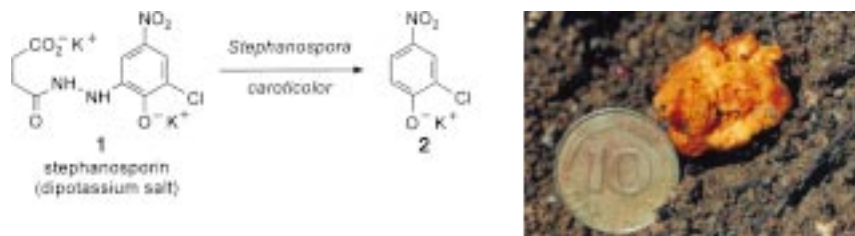
*Angew. Chem.* **2001**, *113*, 1745–1748

R. W. Saalfrank,\* I. Bernt, F. Hampel ..... 1700–1703

Metallacoronates or One-Dimensional Polymers through Self-Assembly—Influence of Templates and Hydrogen Bonding on Product Formation

**Keywords:** coordination chemistry • copper • hydrogen bonds • metallacrown ethers • supramolecular chemistry

**More like an industrial fungicide than a natural product** is the title compound, which occurs as the potassium salt in the carrot truffle, *Stephanospora caroticolor*, and is responsible for its orange color (see picture). On injury of the fruit body, **1** is transformed into the toxic 2-chloro-4-nitrophenol (**2**) by loss of the side chain.



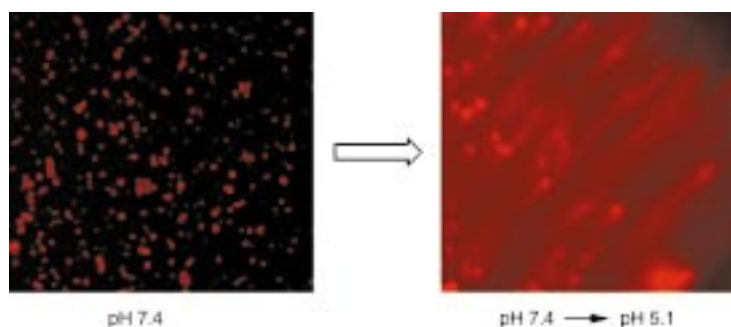
*Angew. Chem.* **2001**, *113*, 1749–1751

M. Lang, P. Spiteller, V. Hellwig, W. Steglich\* ..... 1704–1705

Stephanosporin, a “Traceless” Precursor of 2-Chloro-4-nitrophenol in the Gasteromycete *Stephanospora caroticolor*

**Keywords:** fungi • natural products • nitro compounds • organochloro compounds • phenols

**Microspheres formed from a new poly( $\beta$ -amino ester)** degrade slowly at pH 7.4 (left fluorescence microscopy image) but dissolve quickly at pH values below 6.5 (right), to release encapsulated material rapidly and quantitatively. As the pH/solubility transition occurs within the intracellular pH range, these tiny spheres hold promise as intracellular drug delivery vehicles.



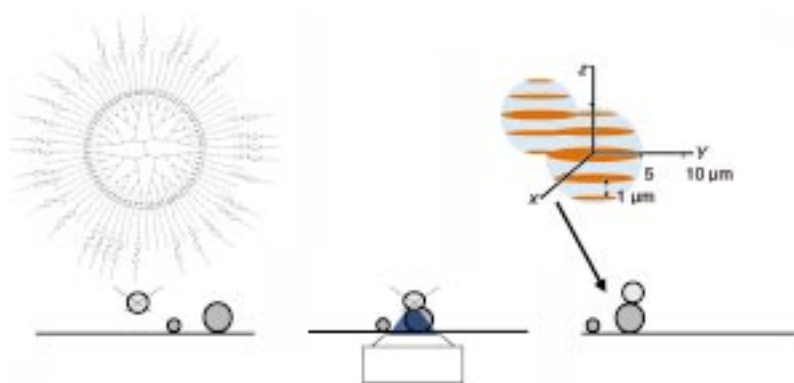
*Angew. Chem.* **2001**, *113*, 1757–1760

D. M. Lynn, M. M. Amiji,  
R. Langer\* ..... 1707–1710

pH-Responsive Polymer Microspheres:  
Rapid Release of Encapsulated Material  
within the Range of Intracellular pH

**Keywords:** controlled release •  
drug research • microspheres •  
polymers • protonation

**Micrometer-level billiards** or rod-formation: The careful design of poly(propyleneimine) dendrimers enables the physical properties of self-assembled vesicular structures to be tuned so that they behave as hard spheres that either undergo collision in a billiardlike manner or merge (see picture).



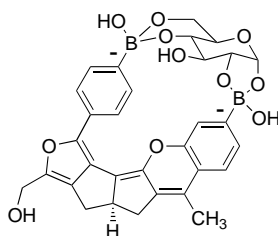
*Angew. Chem.* **2001**, *113*, 1760–1764

G. C. Dol, K. Tsuda, J.-W. Weener,  
M. J. Bartels, T. Asavei, T. Gensch,  
J. Hofkens, L. Latterini,  
A. P. H. J. Schenning, B. W. Meijer,  
F. C. De Schryver\* ..... 1710–1714

Merging of Hard Spheres by  
Phototriggered Micromanipulation

**Keywords:** dendrimers •  
photochemistry • self-assembly • vesicles

**Greater than 400-fold selectivity** for glucose over galactose, mannose, and fructose has been achieved with a receptor designed by the computer program CAVEAT. The receptor has precisely positioned boronic acid groups for cyclic boronate formation with the 1,2- and 4,6-hydroxy groups of  $\alpha$ -D-glucopyranose (see picture) and exhibits a 50% decrease in fluorescence upon glucose binding.




*Angew. Chem.* **2001**, *113*, 1764–1768

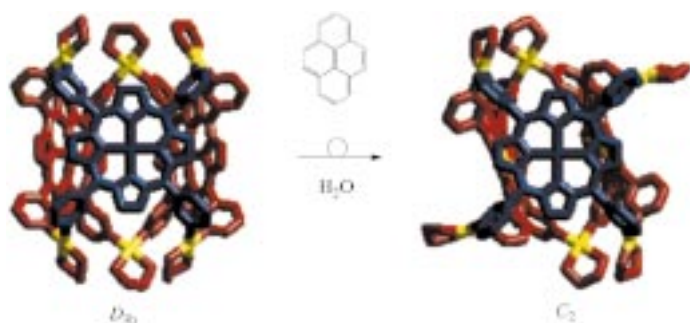
W. Yang, H. He,  
D. G. Drueckhammer\* ..... 1714–1718

Computer-Guided Design in Molecular  
Recognition: Design and Synthesis of a  
Glucopyranose Receptor

**Keywords:** boron • molecular modeling •  
molecular recognition • receptors •  
sensors



 **A prismlike hollow structure** was assembled when three pyridyl-substituted porphyrin panels were linked by six Pd<sup>II</sup> ions. A dramatic  $D_{3h} \rightarrow C_2$  structural change of the prism (see scheme) was triggered by complexation of pyrene.




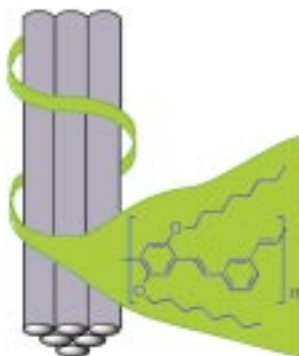
*Angew. Chem.* **2001**, *113*, 1768–1771

N. Fujita, K. Biradha, M. Fujita,\*  
S. Sakamoto, K. Yamaguchi 1718–1721

A Porphyrin Prism: Structural Switching  
Triggered by Guest Inclusion

**Keywords:** host–guest systems •  
palladium • porphyrinoids •  
self-assembly • supramolecular chemistry

 **Intimate electrical contact** occurs between a substituted poly(metaphenylenevinylene) (PmPV) and bundles of single-walled nanotubes (SWNT) as evidenced by atomic force microscopy, optical, and electronic measurements carried out on single, isolated SWNT/PmPV structures (see picture). PmPV may provide a useful route toward “functionalizing” the SWNT without destroying their electrical character.



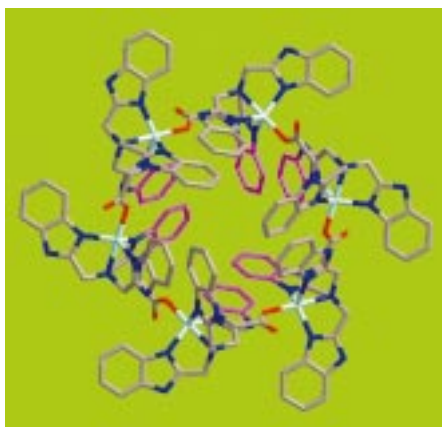
*Angew. Chem.* **2001**, *113*, 1771–1775

A. Star, J. F. Stoddart,\* D. Steuerman,  
M. Diehl, A. Boukai, E. W. Wong,  
X. Yang, S.-W. Chung, H. Choi,  
J. R. Heath\* ..... 1721–1725

Preparation and Properties of Polymer-  
Wrapped Single-Walled Carbon  
Nanotubes

**Keywords:** atomic force microscopy •  
conducting materials •  
molecular devices • nanotubes •  
supramolecular chemistry

**A hexanuclear flying saucer**,  $[\text{Cu}_6(\text{Acntb})_6]^{6+}$  (see structure), is obtained by the reaction of  $\text{Cu}(\text{ClO}_4)_2 \cdot 6\text{H}_2\text{O}$  with the sodium salt of the tripodal ligand  $\text{Acntb}^-$ . Inter-molecular hydrogen bonding generates an open three-dimensional nanoporous network containing intra- and intermolecular cavities of different polarity for guest inclusion.  $\text{HAcntb} = N$ -[ $N'$ -(carboxymethyl)benzimidazol-2-ylmethyl]- $N,N$ -bis(benzimidazol-2-ylmethyl)amine.



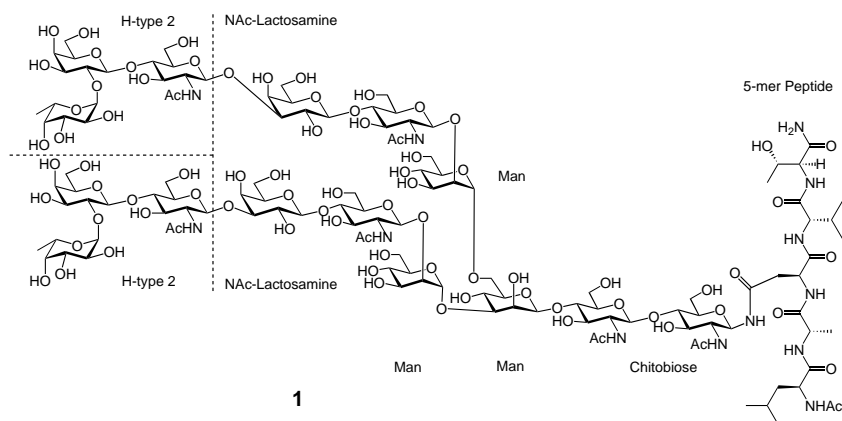
*Angew. Chem.* **2001**, *113*, 1775–1778

C.-Y. Su, X.-P. Yang, B.-S. Kang,\*  
T. C. W. Mak\* ..... 1725–1728

$T_h$ -Symmetric Nanoporous Network Built  
of Hexameric Metallamacrocycles with  
Disparate Cavities for Guest Inclusion

**Keywords:** copper • hydrogen bonds •  
macrocycles • N ligands •  
supramolecular chemistry

**Blood typing** with the ABO classification is based on cell-surface glycoproteins. In a significant step toward the synthesis of these compounds, the laboratory synthesis of a fully functional N-linked glycopeptide featuring H-type blood group determinants **1** is described.



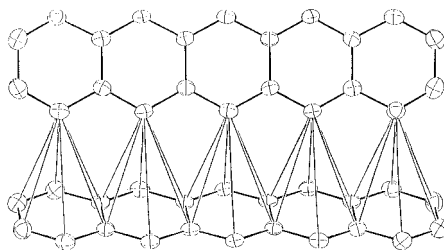
*Angew. Chem.* **2001**, *113*, 1778–1782

Z.-G. Wang, X. Zhang, M. Visser,  
D. Live, A. Zatorski, U. Iserloh,  
K. O. Lloyd,  
S. J. Danishefsky\* ..... 1728–1732

**Toward Fully Synthetic Homogeneous Glycoproteins: A High Mannose Core Containing Glycopeptide Carrying Full H-Type2 Human Blood Group Specificity**

**Keywords:** antibodies • glycals • glycopeptides • glycosylamines • total synthesis

**A low temperature mobility up to  $10\,000\text{ cm}^2\text{ V}^{-1}\text{ s}^{-1}$**  at 1.7 K was observed for a new polymorphic form of pentacene ( $\text{C}_{22}\text{H}_{14}$ , see picture). Optical measurements show a band gap of the order of 2 eV, and transport measurements revealed a mobility above  $3\text{ cm}^2\text{ V}^{-1}\text{ s}^{-1}$  at room temperature.



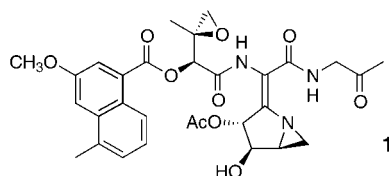
*Angew. Chem.* **2001**, *113*, 1782–1786

T. Siegrist,\* C. Kloc, J. H. Schön,  
B. Batlogg, R. C. Haddon, S. Berg,  
G. A. Thomas ..... 1732–1736

**Enhanced Physical Properties in a Pentacene Polymorph**

**Keywords:** arenes • crystal growth • polymorphism • semiconductors

**A most elusive of synthetic targets**, azinomycin A **1** has now been synthesized for the first time. Using a modular synthetic approach, and after considerable developmental effort, this antitumor agent has been synthesized in a stereocontrolled manner using a convergent series of fragment couplings and a final cyclization to form the structurally unique aziridino[1,2-*a*]pyrrolidine ring system.



*Angew. Chem.* **2001**, *113*, 1786–1789

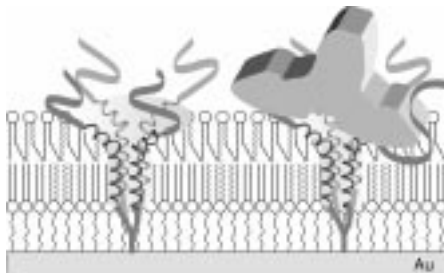
R. S. Coleman,\* J. Li,  
A. Navarro ..... 1736–1739

**Total Synthesis of Azinomycin A**

**Keywords:** antitumor agents • asymmetric synthesis • natural products • peptides • total synthesis



**Specific binding of an antibody** to its antigen at subnanomolar concentrations has been detected electrically by impedance spectroscopy through changes in the ion-conductance of a synthetic ligand-gated ion channel (SLIC) in a supported lipid bilayer on a gold electrode (see picture).



*Angew. Chem.* **2001**, *113*, 1790–1793

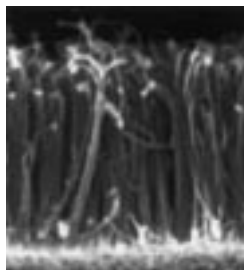
S. Terrettaz, W.-P. Ulrich, R. Guerrini,  
A. Verdini, H. Vogel\* ..... 1740–1743

**Immunosensing by a Synthetic Ligand-Gated Ion Channel**

**Keywords:** antibodies • impedance spectroscopy • lipid bilayers • peptides • receptors



**Fluoroalkylsilane treatment** of super-hydrophobic, aligned carbon nanotube films (see electron micrograph) prepared by pyrolysis of metal phthalocyanines results in the films having both super-hydrophobic and super-lipophobic properties, namely they are super-“amphiphobic” surfaces.



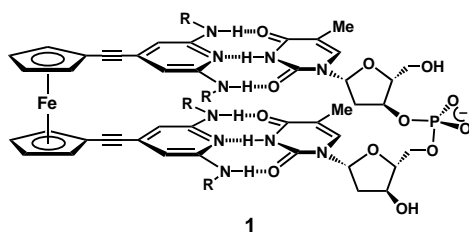
*Angew. Chem.* **2001**, *113*, 1793–1796

H. Li, X. Wang, Y. Song, Y. Liu, Q. Li, L. Jiang,\* D. Zhu ..... 1743–1746

Super-“Amphiphobic” Aligned Carbon Nanotube Films

**Keywords:** carbon • electron microscopy • nanostructures • surface chemistry • wettability

**The multipoint hydrogen-bonded complex 1** (R = alkanoyl) is readily formed between a ferrocene-modified artificial receptor and a dinucleotide. This principle can be used effectively in highly selective, large-scale separations of dinucleotides from mixtures of mono- and oligonucleotides. The process is economically viable and environmentally friendly.



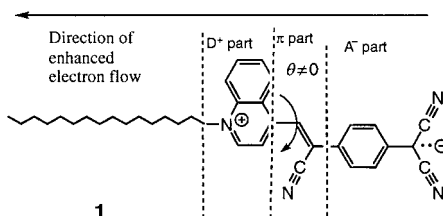
M. Inouye,\* M. Takase ..... 1746–1748

Specific Binding and Separation of Dinucleotides by Ferrocene-Modified Artificial Receptors

**Keywords:** hydrogen bonds • molecular recognition • nucleobases • nucleotides • receptors

*Angew. Chem.* **2001**, *113*, 1796–1798

**45000 electrons per molecule** per second: such currents and a rectification ratio of 5.38 at 2.2 V were detected between oxide-free Au electrodes for a Langmuir–Blodgett monolayer of the D<sup>+</sup>– $\pi$ –A<sup>−</sup> molecule **1**.



T. Xu, I. R. Peterson, M. V. Lakshmikantham, R. M. Metzger\* ..... 1749–1752

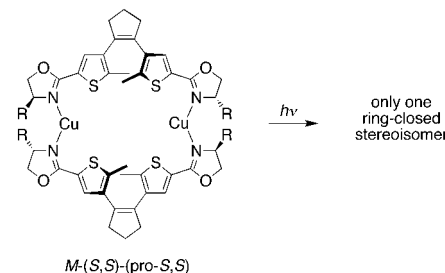
Rectification by a Monolayer of Hexadecylquinolinium Tricyanoquinodimethanide between Gold Electrodes

**Keywords:** conducting materials • donor–acceptor systems • gold • monolayers • rectification

*Angew. Chem.* **2001**, *113*, 1799–1802



**Diastereoselectivities as high as 98%** were the result of the photochemical ring-closure of stereochemically pure copper(I) helicates of a chiral oxazoline-substituted 1,2-dithienylethene photochrome (see scheme). The variations in optical rotation that accompany the photochromic event provide a means to read stored information in a non-destructive manner.



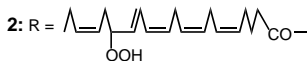
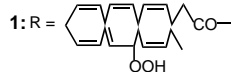
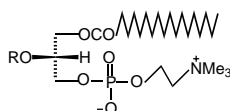
E. Murguly, T. B. Norsten, N. R. Branda\* ..... 1752–1755

Nondestructive Data Processing Based on Chiroptical 1,2-Dithienylethene Photochromes

**Keywords:** diastereoselectivity • helical structures • molecular devices • optical memory • photochromism

*Angew. Chem.* **2001**, *113*, 1802–1805

**The antitumor and antimalarial activity** of fish oils may involve the action of phospholipid hydroperoxides. Two such phosphatidylcholines, **1** and **2**, bearing the hydroperoxides of docosahexaenoic and eicosapentaenoic acids—the two major fatty acids in fish oils—have been synthesized. In spite of its high degree of unsaturation, **1** is sufficiently stable to permit its use in biological studies.



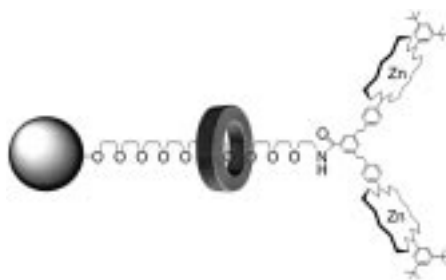
A. N. Onyango, T. Inoue, S. Nakajima, N. Baba,\* T. Kaneko, M. Matsuo, S. Shimizu ..... 1755–1757

Synthesis and Stability of Phosphatidylcholines Bearing Polyenoic Acid Hydroperoxides at the sn-2 Position

**Keywords:** fatty acids • lipids • peroxides

*Angew. Chem.* **2001**, *113*, 1805–1807

**A tricyclic polyamide receptor threads** onto the polyethylene glycol chain of a carbohydrate-attached resin, as shown by gel-phase MAS NMR spectroscopy. This observation led to syntheses of a polymer-supported pseudorotaxane and a porphyrin-stoppered rotaxane (see picture).



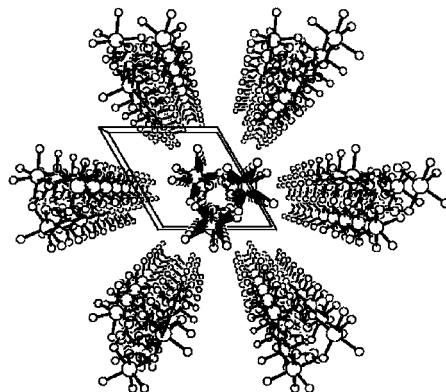
Y.-F. Ng, J.-C. Meillon, T. Ryan,  
A. P. Dominey, A. P. Davis,  
J. K. M. Sanders\* ..... 1757–1760

Gel-Phase MAS NMR Spectroscopy of a Polymer-Supported Pseudorotaxane and Rotaxane: Receptor Binding to an “Inert” Polyethylene Glycol Spacer

**Keywords:** carbohydrates •  
NMR spectroscopy • rotaxanes •  
supramolecular chemistry

*Angew. Chem.* **2001**, *113*, 1807–1810

**Slow magnetic relaxation** and hysteresis effects of dynamic origin have been observed above liquid helium temperature in a chain compound (see picture), comprising  $\text{Co}^{\text{II}}$  centers and organic radicals, without any evidence of phase transition to three-dimensional magnetic order. These results are the first evidence of the slow dynamics predicted for one-dimensional magnetic systems with Ising anisotropy, and they open the possibility of storing information in a single magnetic nanowire.



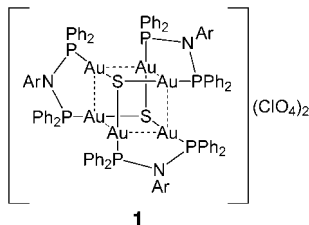
A. Caneschi, D. Gatteschi,\* N. Lalioti,  
C. Sangregorio, R. Sessoli, G. Venturi,  
A. Vindigni, A. Rettori, M. G. Pini,  
M. A. Novak ..... 1760–1763

Cobalt(II)-Nitronyl Nitroxide Chains as Molecular Magnetic Nanowires

**Keywords:** bistability • chain structures •  
cobalt • magnetic properties • radicals

*Angew. Chem.* **2001**, *113*, 1810–1813

**A 1.87-eV energy gap** between the lowest energy excitation maximum and the emission maximum in solution was found for the novel hexanuclear gold(I) sulfido complex **1** ( $\text{Ar} = p\text{-CH}_3\text{C}_6\text{H}_4$ ), which has a heterocubane-type structure. Besides this abnormally large Stokes shift of around  $15000\text{ cm}^{-1}$ , **1** exhibits intense orange luminescence in the solid state.



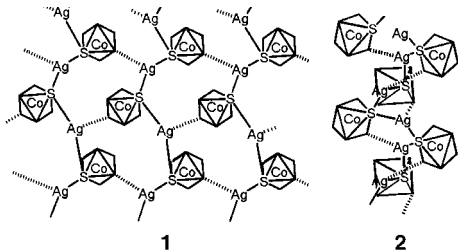
V. W.-W. Yam,\* E. C.-C. Cheng,  
N. Zhu ..... 1763–1765

A Novel Polynuclear Gold–Sulfur Cube with an Unusually Large Stokes Shift

**Keywords:** cluster compounds • gold •  
luminescence • P ligands • sulfur

*Angew. Chem.* **2001**, *113*, 1813–1815

**Sheetlike and helical coordination polymers**,  $\{\Delta_L\text{-[Ag[Co(L-cys-}N,S\text{)-(en)}_2\text{] (NO}_3)_2\}_\infty$  (**1**) and  $\{\Delta_L\text{-[Ag[Co(L-cys-}N,S\text{)-(en)}_2\text{] (NO}_3)_2\}_\infty$  (**2**), were obtained by treating  $\Delta_L$ - and  $\Delta_L\text{-[Co(L-cys-}N,S\text{)-(en)}_2\text{]}^+$  (L-cys = L-cysteinate, en =  $\text{H}_2\text{NCH}_2\text{CH}_2\text{NH}_2$ ) with  $\text{AgNO}_3$  in water, respectively. Their structures are comparable to those of the  $\beta$ -sheet and  $\alpha$ -helix forms of proteins. Compound **2** undergoes reversible conversion into a third compound on changing the pH of the solution.



T. Konno,\* T. Yoshimura, K. Aoki,  
K. Okamoto, M. Hirotsu .... 1765–1768

First Diastereomerically Controlled Aggregation of L-Cysteinato Cobalt(III) Octahedra, Assisted by Silver(I) Ions

**Keywords:** cobalt • helical structures •  
S ligands • silver •  
supramolecular chemistry

*Angew. Chem.* **2001**, *113*, 1815–1818

**Most hydrogenase enzymes have organometallic active sites** with CO and  $\text{CN}^-$  as ligands and metal–metal bonds. Recent evidence points to a novel 2-aza-1,3-propanedithiolate cofactor that directly participates in the heterolytic processing of dihydrogen. A close analogue of this cofactor and its organometallic subunit has been synthesized (see picture); spectroscopic, structural, and theoretical analysis of this model provides detailed insights into the properties of the proposed enzyme active site.



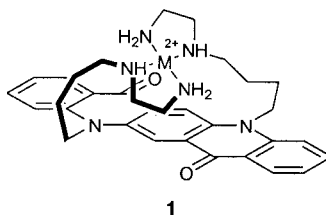
*Angew. Chem.* **2001**, *113*, 1818–1821

J. D. Lawrence, H. Li, T. B. Rauchfuss,\*  
M. Bénard,\* M.-M. Rohmer 1768–1771

Diiron Azadithiolates as Models for the  
Iron-Only Hydrogenase Active Site:  
Synthesis, Structure, and  
Stereoelectronics

**Keywords:** anomeric effect • cyanides •  
density functional calculations •  
hydrogenases • S ligands

**A high-throughput fluorescence assay** for amidases is demonstrated. It illustrates a new principle in enzyme assays, whereby changes in the pM value during the reaction are recorded ( $\text{pM} = -\lg[\text{M}]$ , M = free metal ions). An orange fluorescent quinacridone-based ligand **1** is the pM sensor (shown chelated to a reporter metal ion,  $\text{M}^{2+} = \text{Cu}^{2+}$  or  $\text{Ni}^{2+}$ ) that is used to monitor the release of metal-chelating amino acids by the enzymes acylase I and aminopeptidase.



*Angew. Chem.* **2001**, *113*, 1821–1823

G. Klein, J.-L. Reymond\* ... 1771–1773

An Enzyme Assay Using pM

**Keywords:** enzyme catalysis •  
fluorescence • hydrolysis •  
metal complexes • sensors

**The irreversible formation** of carbonic anhydrase inhibitors from competing building block precursors is templated by the active site of the enzyme itself. The reagents are brought into close proximity of each other in a ternary complex with the enzyme (see scheme).



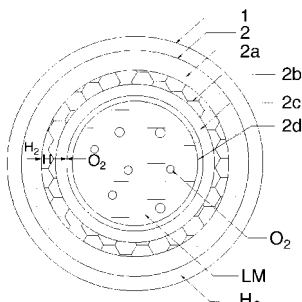
*Angew. Chem.* **2001**, *113*, 1824–1826

R. Nguyen, I. Huc\* ..... 1774–1776

Using an Enzyme's Active Site To  
Template Inhibitors

**Keywords:** drug research •  
enzyme inhibitors • imprinting •  
molecular recognition •  
template synthesis

**Nonhazardous and highly selective  $\text{H}_2\text{O}_2$  production!** An  $\text{H}_2$ -permselective membrane (2) has been developed which consists of thin films of Pd–Ag alloy (2b) and oxidized Pd (2c), and a hydrophobic polymer membrane (2d) supported on a tubular reactor wall (1). Hydrogen atoms permeate through the membrane and react with molecular  $\text{O}_2$  in a liquid medium (LM; 2M  $\text{H}_2\text{SO}_4$ ).



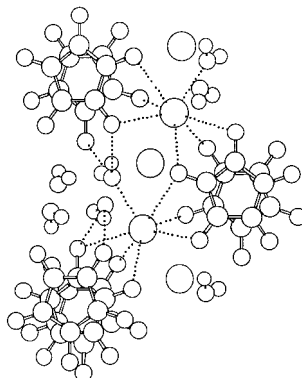
*Angew. Chem.* **2001**, *113*, 1826–1829

V. R. Choudhary,\* A. G. Gaikwad,  
S. D. Sansare ..... 1776–1779

Nonhazardous Direct Oxidation of  
Hydrogen to Hydrogen Peroxide Using a  
Novel Membrane Catalyst

**Keywords:** heterogeneous catalysis •  
membrane reactors • oxidation •  
palladium • peroxides

**Stacks of croconate dianions** separated by  $K^+$  ions and  $H_2O$  molecules: the crystal structure of potassium croconate dihydrate,  $K_2(C_5O_5) \cdot 2H_2O$ , isolated and described by Leopold Gmelin more than 170 years ago, has now been established by X-ray analysis (see picture). Since the anions have a formal charge of  $-2$  and an interplanar separation of only  $3.30 \text{ \AA}$ , the structure is not easily explained in terms of a simple ionic model.



J. D. Dunitz,\* P. Seiler,  
W. Czechtizky ..... 1779–1780

Crystal Structure of Potassium Croconate Dihydrate, after 175 Years

**Keywords:** croconates • hydrates • oxocarbons • potassium • structure elucidation

*Angew. Chem.* **2001**, *113*, 1829–1830



Supporting information on the WWW  
(see article for access details).

\* Author to whom correspondence should be addressed



## BOOKS

<b>Handbook of Ceramic Hard Materials</b>	Ralf Riedel	<i>H. Huppertz</i> ..... 1781
<b>X-Ray Characterization of Materials</b>	Eric Lifshin	<i>P. Dürichen</i> ..... 1782
<b>Phosphorus 2000</b>	Derek E. C. Corbridge	<i>N. W. Mitzel</i> ..... 1783
<b>Organic Conformational Analysis and Stereochemistry from Circular Dichroism Spectroscopy</b>	David A. Lightner, J. E. Gurst	<i>V. Buss</i> ..... 1784
<b>Catalysis from A to Z</b>	Boy Cornils, W. A. Herrmann, R. Schlögl, C.-H. Wong	<i>L. Heinrich</i> ..... 1785
<b>Rhodium Catalyzed Hydroformylation</b>	Piet W. N. M. van Leeuwen, C. Claver	<i>B. Cornils</i> ..... 1785
<b>Iron Metabolism</b>	Glória C. Ferreira, J. J. G. Moura, R. Franco	<i>A. Liu, L. Que, Jr.</i> ..... 1786



## WEB SITES

<a href="http://www.solgel.com">http://www.solgel.com</a> <a href="mailto:prassasm@corning.com">prassasm@corning.com</a>	The Virtual Gateway to Sol–Gel Science	<i>N. Hüsing</i> ..... 1787
---	--	-----------------------------

## SERVICE

• <b>VIPs</b>	<b>1560</b>	• <b>Authors</b>	<b>1785</b>
• <b>Contents of Chemistry—<i>A European Journal</i></b>	<b>1575</b>	• <b>Preview</b>	<b>1786</b>
• <b>Keywords</b>	<b>1784</b>	• <b>Sources</b>	<b>A61</b>

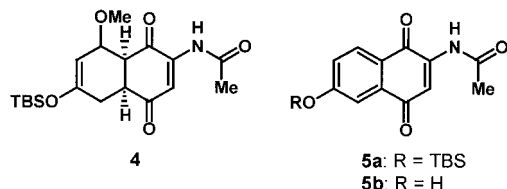
Issue 8, 2001 was published online on April 17, 2001.

Don't forget all the Tables of Contents from 1995 onwards may be still found on the WWW under:  
<http://www.angewandte.com>

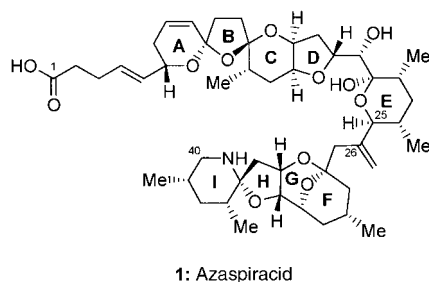


In the communication by **S. H. Bergens** and **V. Rautenstrauch** et al. in issue 5, pp. 914–919, Equations (4) and (6) incorrectly depict (*S*)-(–)-BINAP instead of (*R*)-(+)-BINAP. (*R*)-(+)-BINAP, correctly labeled (+)-**9**, was exclusively used in this work as described in the text. The labels (+)-**9** · HBF<sub>4</sub>, **12**, **13a**, **b**, and **17** in the text and Equation (4) and (6) also correctly refer to the (*R*)-(+)-BINAP series.

In the communication by **K. C. Nicolaou** et al. in issue 1, pp. 207–210, the structures tentatively assigned to compounds **4**, **5a** and **5b** based on NMR spectroscopy were incorrect. The correct structures have now been confirmed by X-ray crystallographic analysis (see picture). We thank Professor Ross Kelly and Professor Antonio Echavarren for inducing us to reexamine this issue (see also T. R. Kelly, M. Behforouz, A. Echavarren, J. Vaya, *Tetrahedron Lett.* **1983**, 24, 2331–2334).



In the communication by **K. C. Nicolaou** et al., in issue 7, pp. 1262–1265, the structure of the title compound azaspiracid (**1**) was inadvertently depicted incorrectly at three stereocenters. The correct structure is shown below.



The IR data for compound **3** are as follows:  $\tilde{\nu}_{\text{max}} = 2925, 2861, 1697, 1460, 1373, 1255, 1149, 597 \text{ cm}^{-1}$ .